

Synthesis and Properties of Photochromic Cholesteric Liquid Crystalline Polysiloxane Containing Chiral Mesogens and Azobenzene Photochromic Groups

JUNGE ZHI, BAOYAN ZHANG, BAOLING ZANG, GUOHUA SHI

Department of Chemistry, Northeastern University, Shenyang 110004, People's Republic of China

Received 27 May 2001; accepted 12 October 2001

ABSTRACT: A series of novel thermotropic side-chain liquid crystalline polymers (P_0 – P_{12}) were synthesized by grafting copolymerization of mesogenic monomer cholesteryl undecylenate (M1) and photochromic monomer 4-allyloxy-4'-nitroazobenzene (M2) on polymethylhydrosiloxane. The chemical structures of polymers were characterized by infrared (IR) and ultraviolet (UV) spectroscopy. Differential scanning calorimetry (DSC) and thermogravimetric analysis (TGA) were used to measure the thermal properties of those polymers, and the mesogenic properties were characterized by polarized optical micrograph, DSC, wide-angle X-ray diffraction and small-angle X-ray scattering. The glass transition temperatures (T_g 's) of the polymers increased from P_0 to P_4 and decreased from P_5 to P_{12} . The clearing point temperatures (T_i 's) of the polymers P_1 – P_{12} were lower than that of P_0 , but increased from P_1 to P_4 and decreased from P_5 to P_{12} . They showed thermotropic liquid crystalline properties in a broad mesogenic region at temperatures $>100^\circ\text{C}$. The polymers P_0 – P_8 exhibited a cholesteric mesophase with oily streaks and lined texture, and polymers P_9 – P_{12} showed a chiral smectic mesogenic phase with a layered texture. All of the polymers were thermally stable to $\sim 320^\circ\text{C}$. The UV-induced *trans*–*cis* photoisomerization was investigated for the azo monomer and polymers P_8 and P_{12} . The solution of the azo monomer and liquid crystalline polymers P_8 and P_{12} can undergo photoisomerization, and the environments of the azo group were responsible for the aforementioned photochemical process. © 2002 Wiley Periodicals, Inc. *J Appl Polym Sci* 85: 2155–2162, 2002

Key words: cholesteric mesophase; smectic; oily streak texture; azobenzene; photochromism

INTRODUCTION:

In recent years, much attention has been paid to the reversible and irreversible photochromic chiral liquid crystalline polymer systems for optical applications, such as data storage and display devices.^{1–3} And there has been a growing interest in developing materials exhibiting both liquid

crystalline properties and photochromism.^{3–7} Now menthone, azobenzene, diaryrethenes, and fulgides derivatives have been reported for reversible and irreversible thermotropic chiral liquid crystalline polymer systems.⁷ Moreover, chiral low-molar-mass liquid crystalline systems containing other photochromic compounds, such as spironaphthoxazine, spiropyran, helical alkene, and thioindigos, have also been reported.^{7,8} These reports indicated that liquid crystalline polymer materials containing reversible or irreversible dyes can not only be used in optical information

Correspondence to: B-Y. Zhang (baoyanzhang@hotmail.com).

Journal of Applied Polymer Science, Vol. 85, 2155–2162 (2002)
© 2002 Wiley Periodicals, Inc.

storage by light-induction, but also exhibit many excellent properties,^{9,10} such as little energy needed when storing, storing repeatedly, storing for long time, high sharpness of separation, and so on. Now, many researchers pay more attention to the thermotropic liquid crystalline polymers containing azobenzene for their special properties and use for reversible and irreversible polymer systems.⁵⁻⁷

It is well known that siloxane polymers are materials of significant technological interest. The siloxane bond (Si—O) offers a highly flexible structure unit, yielding polymer chains with low glass temperature (T_g) and surface tensions, and unique physical and chemical properties.⁸ In the present article, a series of photochromic liquid crystalline polymers (P_0 – P_{12}) consisting of an azobenzene-containing monomeric unit with a propylene spacer and a cholesterol-containing monomeric unit with an undecamethylene spacer were synthesized. The thermotropic liquid crystalline properties, the textures, and the effect of the structure of the azobenzene monomeric unit on the phase behaviors of the photochromic liquid crystalline polymers P_0 – P_{12} are discussed, and the photochromic properties of the polymers are explored.

EXPERIMENTAL

Reagents and Intermediates

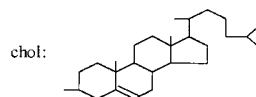
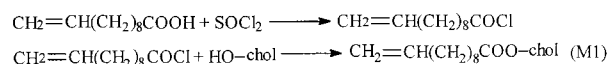
Polymethylhydrosiloxane (PMHS), with MW of 700–800, was supplied by Jilin Chemical Industry Company (Jilin Province, PRC), and cholesterol was supplied by Xiayi Biochemistry Medicine Company (Hunan Province, PRC). Toluene was distilled after being dried with CaCl_2 for 24 h. Tetrahydrofuran (THF) was predried with molecular sieves, refluxed over lithium hydride, and then distilled. Allyl bromide was distilled before being used. Undecylenic acid, thionyl chloride, *N,N*-dimethylbenzeneamine, ether, 4-nitroniline, sodium nitrite, phenol, potassium iodide, sodium sulfonate, methanol, and ethanol were used as received.

Monomer Synthesis

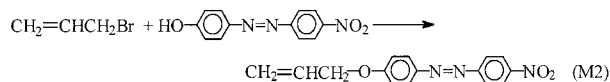
Cholesteryl Undecylenate (M1)

M1 was prepared by the following procedure (see Scheme 1). Undecylenic acid (0.15 mol) and thionyl chloride (0.3 mol) were allowed to react at

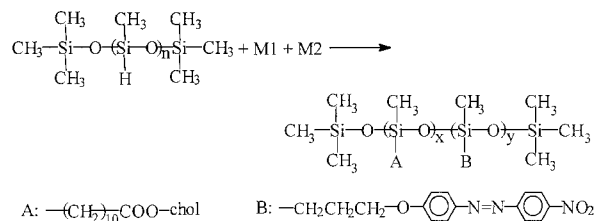
Preparation of Cholesteryl Undecylenate(M1)



Preparation of 4-Allyloxy-4'-nitro azobenzene(M2)



Polymers(P_0 – P_{12}) synthesis



Scheme 1 Synthesis pathways of monomers and polymers.

room temperature for 3 h, and then were refluxed at 60°C for 5 h in a three-necked flask. Finally, the undecylenic chloride was obtained by collecting the fraction of 129–131°C/1.33 KPa. The yield was 78%.

The undecylenic chloride (0.02 mol) and cholesterol (0.01 mol) were dissolved in *N,N*-dimethylbenzeneamine (15 mL) and reacted at 100°C for 2 h. The mixture was then added to cool water (100 mL) and extracted with ether (50 mL). The organic phase was washed with 1.00 mol/L H_2SO_4 and 1.00 mol/L NaHCO_3 , dried with MgSO_4 , and then concentrated. The M1 (mp, 80–81°C) was separated out by filtering, then recrystallized from aqueous ethanol. The yield was 75%; IR (KBr) cm^{-1} : 3056(=C—H), 1734 (C=O), 2881, 2993(— CH_2 —, CH_3 —).

4-Allyloxy-4'-nitroazobenzene (M2)

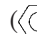
M2 was prepared according to the procedure of Shao.¹⁶ 4-Allyloxy-4'-nitroazobenzene was synthesized according to the following procedure (see Scheme 1). Allyl bromide (0.015 mol) was dripped into ethanol solution of 4-hydroxy-4'-nitroazobenzene (0.01 mol) and a catalytic amount of potas-

Table I Polymerization

Sample	Feed				Polymer		
	PMHS (mol)	M1 (mol)	M2 (mol)	(M1) ^a (mol%)	Yield (%)	$[\alpha]_D^{15}$	Color
M1	—	—	—	—	—	−34.50	white
P ₀	1	7.000	0	100	82.9	−28.79	grayish white
P ₁	1	6.965	0.035	99.5	79.5	−28.00	orange
P ₂	1	6.930	0.070	99.0	81.2	−27.38	orange
P ₃	1	6.895	0.105	98.5	83.3	−26.96	red
P ₄	1	6.860	0.140	98.0	81.0	−26.39	red
P ₅	1	6.790	0.210	97.0	79.5	−26.01	red
P ₆	1	6.720	0.280	96.0	82.3	−25.65	red
P ₇	1	6.650	0.350	95.0	84.3	−24.77	red
P ₈	1	6.300	0.700	90.0	83.4	−22.30	deep red
P ₉	1	5.950	1.050	85.0	79.5	−20.00	deep red
P ₁₀	1	5.600	1.400	80.0	81.5	−17.50	deep red
P ₁₁	1	5.250	1.750	75.0	87.8	−15.57	brown
P ₁₂	1	4.900	2.100	70.0	82.2	−13.24	brown

^a Mole percent of M1 based on M1 + M2.

sium iodide, then the solution was refluxed at 40°C for 12 h. The M2 (mp, 146–148°C) was separated out by cooling the solution and filtering, then recrystallized from ethanol. The product is deep red and the yield was 72%;

IR (KBr) cm^{-1} : 3034 (=C—H), 1601, 1508 ()₆, 1525, 1338 (O=N=O).

Polymer Synthesis

The monomers M1, M2, and PMHS (Table I) were dissolved in toluene (30 mL), a catalytic amount (2 mL) of hydrogenhexchloroplatinate (IV) hydrate/THF solution (the molar ration of Pt/THF was 1/10³) was added to the above solution under nitrogen, and the reaction temperature was 60–70°C (see Scheme 1). The progress was monitored by the disappearance of the Si—H stretch at 2160 cm^{-1} by IR spectroscopy. On completion, the reaction was added into methanol (200 mL) to precipitate the product. The products were washed with methanol repeatedly, and then dried under vacuum.

Characterization Techniques

IR Spectroscopy

The monomers and polymers were characterized by Fourier transform infrared spectroscopy (FT-IR) with a Nicolet 510P FT-IR spectroscope, using all samples on KBr.

UV Spectroscopy

The UV spectra of samples in cyclohexane were measured with a HP6010 UV–visible (UV–vis) spectrometer.

Optical Rotation Analysis

Optical rotation was carried out with Shanghai WZZ-1S digital polarimeter, using toluene as the solvent.

Thermal Analysis

Thermal transitions were measured with a Perkin-Elmer DSC-7 equipped with a PE7300 data station, using a nitrogen atmosphere and a 20°C/min heating rate. The thermal stabilities of the polymers in a nitrogen atmosphere were measured with a Perkin-Elmer TGA-7 thermogravimetric analyzer using a 20°C/min heating rate.

Polarizing Optical Microscope (POM) Analysis

The textures of monomers and polymers were observed with a Ziss-Jena polarizing optical microscope equipped with a Mettler FP2 hot stage.

X-ray Diffraction Analysis

X-ray diffraction analysis of quenched samples was measured with a Rigaku DMAX-3A X-ray

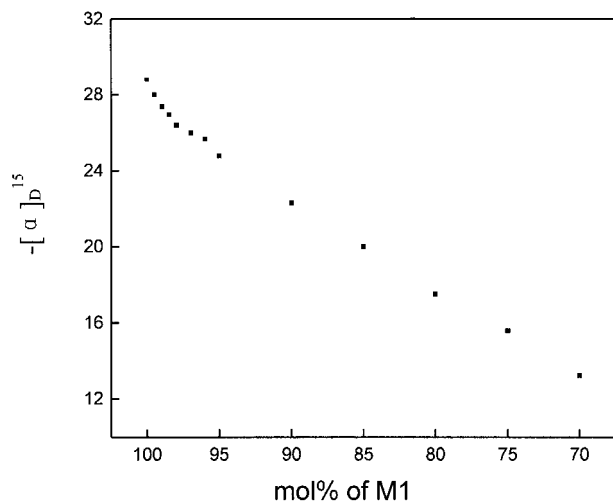


Figure 1 The changing of SRP with concentration of M1 in polymers.

diffractometer at room temperature, with $\text{CuK}\alpha$ radiation.

RESULTS AND DISCUSSION

Polymerization and Chiroptical Properties

The polymerization experiments are summarized in Table I. The progress of the grafting reactions, monitored by the disappearance of the Si—H stretch (2166 cm^{-1}) intensity, was affected by spacer group length and composition. More time is needed for the Si—H to react when increasing the content of M2 with the shorter flexible spacer: $\text{P}_0\text{--P}_5$ had a 100% complete reaction in 50 h, but $\text{P}_{10}\text{--P}_{12}$ took more time. This result indicates that the length of the flexible spacer group had an effect on the reaction.¹¹

All the polymers in toluene solution are optically active at 589 nm, which is analogous to other copolymers.^{12,13} The specific rotatory powers (SRPs) of the polymers, which are negative, are listed in Table I. The SRP of polymer P_0 is lower than that of chiral monomer M1, and the SRP nearly linearly decreases from P_0 to P_{12} . The changing of SRPs of polymers with the concentration of M1, which is consistent with the equation $-[\alpha]_D^{15} = 50C - 22$ (where C is the mole percent of monomer M1), is shown in Figure 1. This result can be explained by Van't Hoff's Optical Rotation Addition Theory.¹⁴ The decrease of the SRP of polymer P_0 in comparison with M1 is attributed to the decreasing of the concentration of optically

active component in P_0 . The SRP decreasing from P_0 to P_{12} is due to the decrease of the content of the optically active mesogen in every polymer molecule when increasing optically inactive monomer M2 in grafting copolymerization.

UV Spectroscopy

The UV-vis absorption spectra of monomer M2 and all of the polymers in the region $\lambda = 290\text{--}500\text{ nm}$ are shown in Figure 2(a). The monomer M1 exhibited no absorption in this wavelength region, but monomer M2 showed a strong absorption maxima at 370–375 nm and a weak absorption at 440–460 nm, which are due, respectively, to the $\pi\text{--}\pi^*$ and $\text{n--}\pi^*$ electronic transitions of azobenzene.^{12,15} Both of the absorption bands shifted to higher wavelength than that of the isolated azo, which is attributed to the conjugative effect of $\text{N}=\text{N}$ and C_6H_5 . Polymer P_0 showed no absorption, like monomer M1, but polymers $\text{P}_1\text{--}$

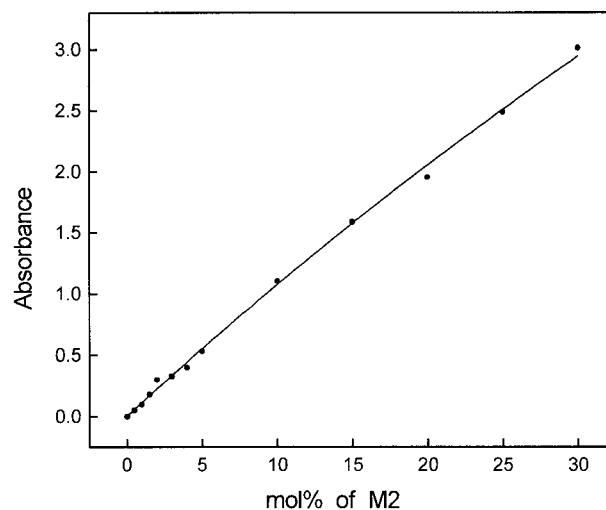
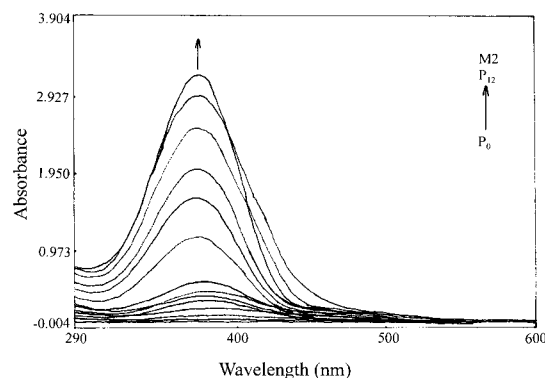


Figure 2 (a) UV absorption spectra of monomer M2 and polymers. (b) Change in absorbance of polymers at 372 nm with concentration of M2.

P₁₂ exhibited absorption peaks at ~ 370 and ~ 450 nm due to the introduction of the conjugated N=N. The absorbance linearly increases when the content of M2 unit increases from 0.5 to 30 mol % in the polymers, which provide evidence for the grafting copolymerization, and the absorbance changing with M2 concentration at $\lambda = 372$ nm is shown in Figure 2(b).

Thermal Analysis

The thermal transitions of the polymers were measured by DSC by first heating the sample to 100°C, then cooling to -50°C after 5 min, and reheating the sample at 20°C/min to 250°C. The second heating scans are shown in Figure 3(a), and the transition temperatures are summarized in Table II. The glass transition temperatures (T_g s) of polymers are at 4–20°C, and T_g increased from P₀ to P₄ and decreased from P₅ to P₁₂, as shown in Figure 3(b). The low T_g s are attributed to the flexible siloxane main-chain and the flexible spacer $-(\text{CH}_2)_n-$ ($n = 10$) between the main-chain and the bulky cholesteryl. The increasing of T_g from P₀ to P₄ is attributed to the introduction of a little rigid azobenzene. The rigidity of the azobenzene mesogen had an effect on T_g , and the effect increased with increasing the concentration of azobenzene; therefore, T_g increased from P₀ to P₄. Moreover, the increase of T_g may be partly due to the microfiber reinforcing effect of a little rigid azobenzene mesogen. But the steric effect of bulky cholesteryl reduced with decreasing the concentration of M1 from P₅, whereas the influence of the rigidity increased with increasing the content of azobenzene mesogen; thus, the T_g s of polymers P₅–P₇ were higher than that of P₀ although T_g decreased from P₅. The steric effect of bulky cholesteryl decreased quickly from P₈, and the effect of the rigidity of azobenzene mesogen could not keep equilibrium with the decrease of the steric effect; therefore, T_g decreased quickly from P₈. The clearing point temperatures (T_i s) of polymers P₁–P₁₂ were lower than that of P₀, and T_i increased from P₁ to P₄, but decreased from P₅ to P₁₂, as shown in Figure 3(b). Both the steric effect of the bulky cholesteryl and the rigidity of the rigid azobenzene mesogen influenced T_i of polymers; the predominating one will determine the changing of T_i . The increase of T_i from P₁ to P₄ is due to the increase the content of rod-shaped azobenzene whose rigidity is beneficial to keeping the alignment of polymer molecule in the liquid crystalline phase. But the steric effect of bulky

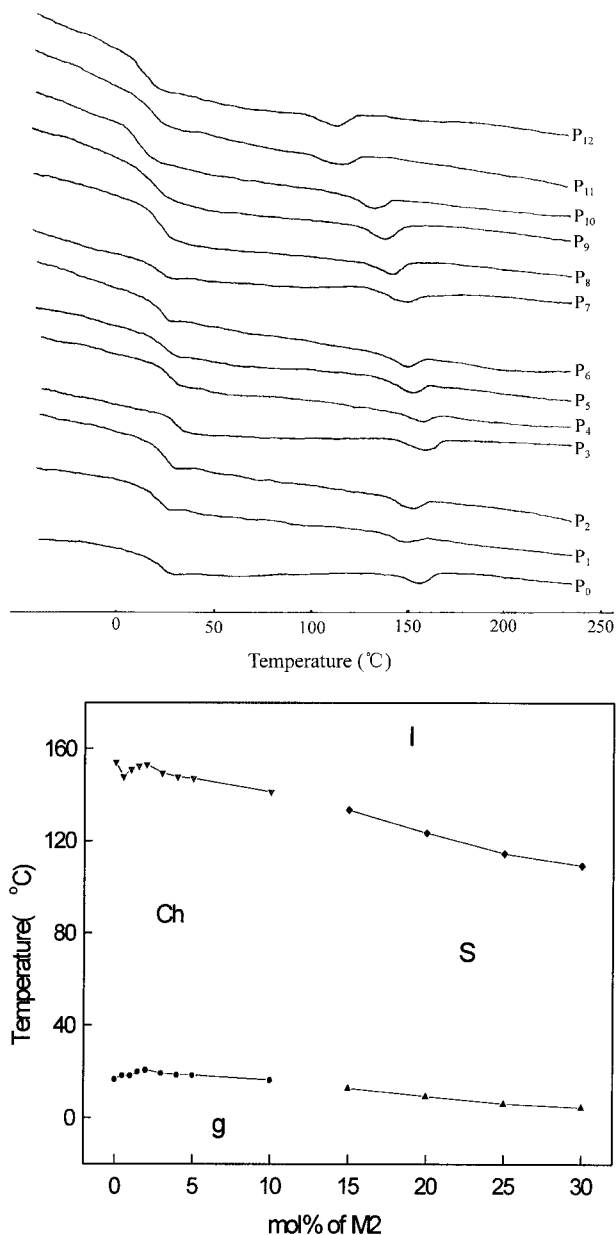


Figure 3 (a) DSC thermograms (second heating) of polymers. (b) Phase transition temperatures of polymers as a function of M2 concentration (I: isotropic; Ch: cholesteric; s: smectic; g: glassy).

cholesteryl predominated from P₅, and the decrease of the effect reduced the energy of disorientation for polymer molecules in the liquid crystalline phase when decreasing the concentration of M1; thus, T_i decreased from P₅ to P₁₂. But the T_i of polymers P₁–P₁₂ decreased 1.1–45.0°C compared with P₀, which is attributed to the introduction of rod-shaped azobenzene. Figure 3(b) exhibits the liquid crystalline mesogenic ranges

Table II Thermal Analysis Results

Polymer	n ^a	DSC					TGA			
		T _g (°C)	T _i (°C)	ΔH _j (J/g)	ΔT ^b (°C)	T _{5%} ^c (°C)	Weight Loss (%)			
							300°C	350°C	425°C	600°C
P ₀	100	16.5	154.1	1.933	137.6	323.6	1.4	18.1	62.6	94.8
P ₁	99.5	18.1	147.8	1.402	129.7	294.7	5.7	24.1	69.4	84.6
P ₂	99.0	18.0	150.9	1.874	132.9	311.2	2.9	26.9	65.9	91.1
P ₃	98.5	19.7	152.4	1.947	132.7	328.3	0.7	12.4	58.7	82.9
P ₄	98.0	20.5	153.0	2.011	132.5	305.1	4.3	20.1	68.2	71.7
P ₅	97.0	19.1	149.3	1.893	130.2	303.0	4.4	24.4	76.9	81.2
P ₆	96.0	18.4	147.6	2.242	129.2	294.9	5.1	26.3	74.0	92.4
P ₇	95.0	18.2	147.0	2.191	128.8	309.5	3.0	30.0	67.1	87.5
P ₈	90.0	16.1	141.1	2.040	125.0	317.5	2.2	21.0	63.7	84.7
P ₉	85.0	12.7	133.3	1.554	120.6	307.1	3.4	30.8	63.6	77.5
P ₁₀	80.0	9.1	123.3	1.868	114.3	297.6	6.6	31.0	67.6	79.6
P ₁₁	75.0	6.0	114.4	1.802	106.4	304.3	2.8	26.9	61.0	72.9
P ₁₂	70.0	4.4	109.1	1.805	104.7	302.6	4.7	27.6	63.7	76.6

^a The mole fraction of monomer M1.

^b The mesomorphic temperature range (i.e., T_i - T_g).

^c Temperature at which 5% loss occurred.

(ΔT (°C) = T_i - T_g) of polymers. They are broader than 100 °C, and decrease from P₀ to P₁₂.

The temperature of 5% mass loss (T_{5%}) occurred and the percent mass loss at various temperatures, determined by TGA,, are summarized in Table II. The T_{5%} of polymers are at >300°C, which indicates that all of the polymers are thermally stable to ~ 300°C.

Texture Analysis

The textures of monomers and polymers observed with POM are shown in Figure 4. All of them exhibited thermotropic liquid crystalline properties in both heating and cooling processes. The monomer M1 exhibited a typical cholesteric focal-conic texture, and monomer M2 showed a typical nematic gravel-shaped texture.¹⁶ In the present article, the polymers P₀-P₈ exhibited cholesteric textures with the lined texture and oily streaks, as shown in Figure 4(a, b). But the polymers P₉-P₁₂ showed layer-shaped texture or lined texture of smectic textures. Figure 4(c) shows a typical smectic texture of polymer P₁₀. These textures will be further identified by X-ray diffraction analysis.

The wide angle X-ray diffraction and small angle X-ray scattering patterns of quenched sam-

ples of the polymers at different temperatures are shown in Figure 5. All of the polymers were amorphous and may exhibit different molecular packing pattern and different liquid crystalline phases, which will be explained by the latter analysis. The wide-angle X-ray diffraction patterns of polymers P₀ and P₁₂ exhibited diffuse peaks at ~ 2θ = 17° and 20°, respectively, as shown in Figure 5(a). No sharp peaks were observed for polymers P₀-P₈ in the lower Bragg angle region, a weak scattering peak at 2θ < 1.5° was noted for polymer P₉, and a sharp peak at 2θ = 0.4° was observed for polymer P₁₂, as shown in Figure 5(b). The corresponding d-spacing of smectic orientations of mesogen indicated that the degree of ordering of the layer structure packed by side-chain polymer increased when the concentration of rod-shaped monomer M2 increased. Thus, polymers P₁-P₈ exhibited a cholesteric mesophase (chiral nematic mesophase) with oily streaks and lined texture, polymers P₉-P₁₂ showed a chiral smectic mesophase with layered texture, and the regularity of polymer molecule improved from P₉ to P₁₂.³ This result provides evidence that a rigid rod-shaped mesogen can accelerate the formation of a layered structure for comb-shaped liquid crystalline polymers and make the polymer exhibit a smectic mesophase.^{17,18}

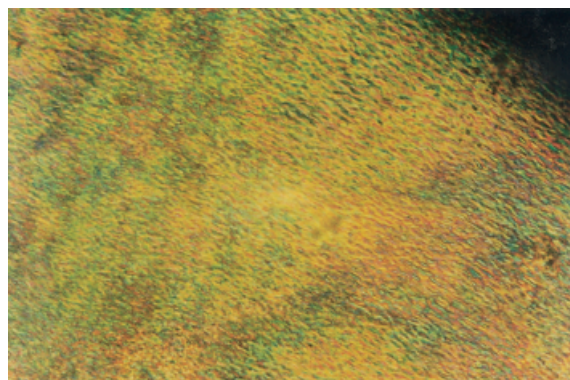
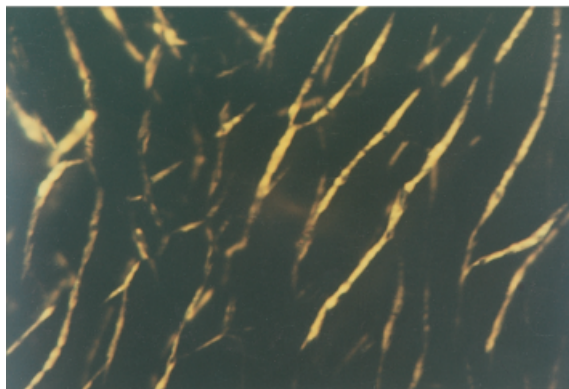
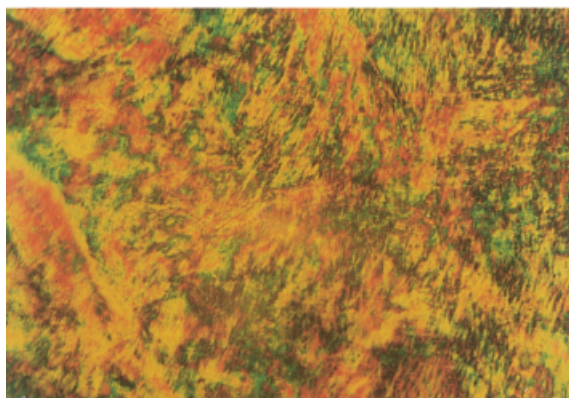
(a) P_0 at 148.5°C (200×)(b) P_5 at 130.3°C (200×)(c) P_{10} at 98°C (200×)

Figure 4 Polarized optical micrograph (200×) of polymers: (a) P_0 at 148.5°C; (b) P_5 at 130.3°C; and (c) P_{10} at 98°C.

Photochemical Characterization of M2 and Polymers

The UV-visible spectral changes on irradiation at 370 nm of polymer P_8 in cyclohexane are shown in Figure 6(a). The absorbance intensity of azo at

372 nm decreased with increasing irradiation time until a photostationary state was reached. This state is due to the azobenzene chromophores undergoing a *trans-cis* photoisomerization process without any side reactions. This process is proved by the existence of isosbestic points at 295–300 and 415–425 nm in the corresponding UV-vis spectra,¹⁵ as shown in Figure 6(a).

The changes in the relative absorbance (A/A_0) dependence on irradiation time is shown in Figure 6(b). The decrease of A/A_0 indicates that the *trans-cis* isomerization rate of M2 is slightly lower in comparison with that of polymer P_{12} , and the *trans-cis* isomerization rate of polymer P_8 is higher than that of polymer P_{12} , as shown in Figure 6(b). These results are due to the decrease of the content of azobenzene in polymers and/or

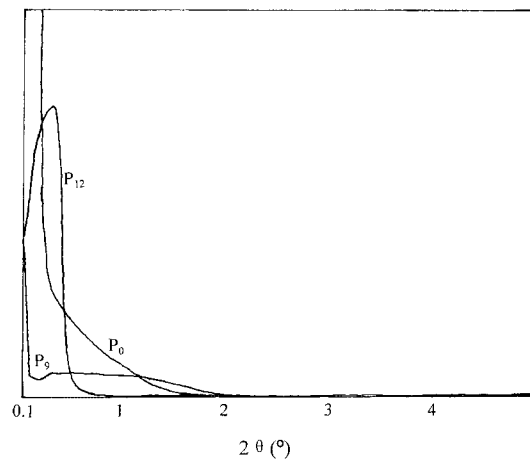
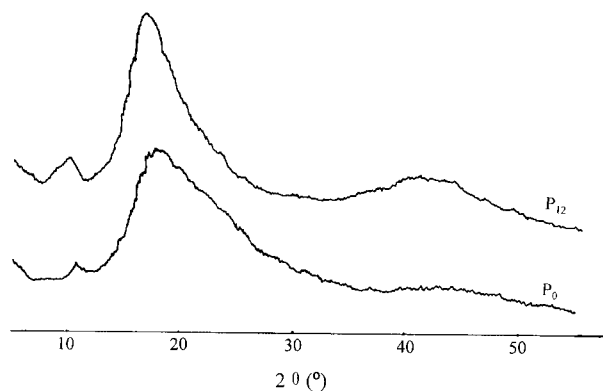


Figure 5 (a) Wide-angle C-ray diffraction patterns of polymers. (b) Small-angle C-ray scattering patterns of polymers.

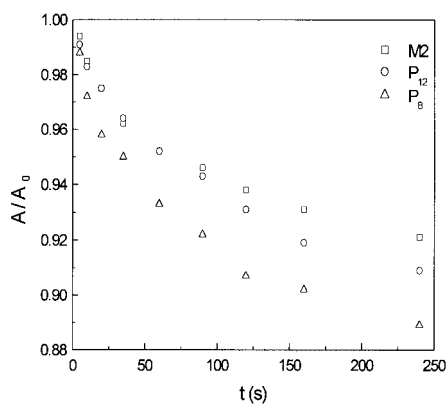
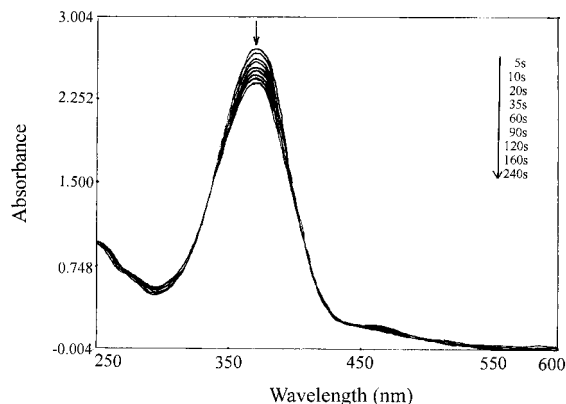


Figure 6 (a) UV-vis spectral change on irradiation (370 nm light) of polymer P_8 in cyclohexane. (b) Decrease in the dependence of the relative absorbance (A/A_0) on irradiation time (irradiation at 370 nm).

the accelerating effect of the chiral groups in the comb-like polymers.^{15–19} The high decrease rate of polymer P_8 may be due to the accelerating effect of the neighboring chiral groups for the molar ratio of azobenzene and chiral group(cholesteryl) is $\sim 1 : 9$ in polymer P_8 . The influence factors on *trans-cis* isomerization of azobenzene are under further investigation.

CONCLUSIONS

Photochromic liquid crystalline polymers (P_0 – P_{12}) containing photochromic monomers and mesogenic monomer cholesteryl undecylenate on the side-chain to the PMHS backbone were synthesized by graft copolymerization. They all exhibit thermotropic liquid crystalline properties and

mesomorphic behavior in a broad temperature range $>100^\circ\text{C}$. Polymers P_0 – P_8 exhibited a cholesteric mesophase with oily streaks and lined texture, and polymers P_9 – P_{12} showed a chiral smectic mesogenic phase with layered texture. The studies of UV-induced *trans-cis* photoisomerization of the azo monomer and polymers P_8 and P_{12} in solution indicated that the solution of the azo monomer and polymers P_8 and P_{12} can undergo photoisomerization.

The authors acknowledge financial support of National Natural Scientific Fundamental Committee of China, the Minister of Science and Technology of China, the Liaoning Provincial Department of Science and Technology and the Science Committee of Shenyang.

REFERENCES

- Petri, A.; Kummer, S.; Brauchle, C. H. *Liq Cryst* 1995, 19, 277.
- Bobrovsky, A. Y.; Boiko, N. I.; Shibaev, V. P. *Liq Cryst* 1998, 25, 393.
- Boiko, N. I.; Kutulya, L. A.; Rezaikovetl, A. Y. *Mol Cryst Liq Cryst* 1994, 251, 311.
- Witte, P.; Galan, J. C. *J Mol Cryst* 1998, 24, 819.
- Kozlovsky, M. V.; Shibaev, V. P.; Stakhanov, A. I.; Haase, W. *Liq Cryst* 1998, 24, 759.
- Saminathan, M.; Pillai, C. K. S. *Polymer* 2000, 41, 3103–3108.
- Hattori, H.; Uryu, T. *J Polym Sci, Part A: Polym Chem* 2000, 38, 887.
- Natarajan, L. V.; Bunning, T. J.; Kim, S. Y. *Macromolecules* 1994, 27, 7248.
- Eich, M.; Wendorff, J. H. *Makromol Chem, Rapid Commun* 1987, 8, 59.
- Hvilsted, S.; Andruaai, F., et al. *Macromolecules* 1995, 28, 2172.
- Mihara, T.; Nomura, K.; Funaki, K. *Polym J* 1994, 29, 309.
- Altomare, A.; Carlini, C.; Panattoni, M. *Macromolecules* 1984, 17, 2207.
- Cabrera, I.; Krongauz, V.; Ringsdorf, H. *Mol Cryst Liq Cryst* 1988, 155, 221.
- Van't Hoff, J. H. *Dielerung der Atome im Raum*, 2nd ed.; Vieweg & Sohn: Braunschweig, 1894; p. 119.
- Niemann, M.; Ritter, H. *Makromol Chem* 1993, 194, 1169.
- Shao, B.; Zhang, B. Y.; Hu, J. S. *Polym Mater Sci Eng*, to appear.
- Zhang, B. Y.; Guo, S. M.; Shao, B. *J Appl Polym Sci* 1998, 168, 1555.
- Zhou, Q. F. *Liquid Crystalline Polymer*; Science Press: Beijing, P. R. China, 1994; p. 63.
- Angiolini, L.; Caretti, D.; Giorgini, L.; Salatelli, E. *Polymer* 2000, 41, 4767.